NRC·CNRC

NRC Publications Archive
Archives des publications du CNRC

The use of attenuated total reflection infrared spectroscopy to study the intercalation of molten polymer into layered silicates in real time

Cole, Kenneth C.

This publication could be one of several versions: author's original, accepted manuscript or the publisher's version. / La version de cette publication peut être l'une des suivantes : la version prépublication de l'auteur, la version acceptée du manuscrit ou la version de l'éditeur.
For the publisher's version, please access the DOI link below./ Pour consulter la version de l'éditeur, utilisez le lien DOI ci-dessous.

Publisher's version / Version de l'éditeur:
https://doi.org/10.1366/000370209790108888
Applied Spectroscopy, 63, 12, pp. 1343-1350, 2009-12-01

NRC Publications Record / Notice d'Archives des publications de CNRC:
https://nrc-publications.canada.ca/eng/view/object/?id=a13772e6-7749-43d3-8fbf-6ae4657d952f
https://publications-cnrc.canada.ca/fra/voir/objet/?id=a13772e6-7749-43d3-8fbf-6ae4657d952f

Access and use of this website and the material on it are subject to the Terms and Conditions set forth at https://nrc-publications.canada.ca/eng/copyright
READ THESE TERMS AND CONDITIONS CAREFULLY BEFORE USING THIS WEBSITE.

L'accès à ce site Web et l'utilisation de son contenu sont assujettis aux conditions présentées dans le site https://publications-cnrc.canada.ca/fra/droits
LISEZ CES CONDITIONS ATTENTIVEMENT AVANT D'UTILISER CE SITE WEB.

Questions? Contact the NRC Publications Archive team at PublicationsArchive-ArchivesPublications@nrc-cnrc.gc.ca. If you wish to email the authors directly, please see the first page of the publication for their contact information.

Vous avez des questions? Nous pouvons vous aider. Pour communiquer directement avec un auteur, consultez la première page de la revue dans laquelle son article a été publié afin de trouver ses coordonnées. Si vous n'arrivez pas à les repérer, communiquez avec nous à PublicationsArchive-ArchivesPublications@nrc-cnrc.gc.ca.

National Research Council Canada | Conseil national de recherches Canada

Canada

IMI 2009-119594-G
CNRC 51088

The Use of Attenuated Total Reflection Infrared Spectroscopy to Study the Intercalation of Molten Polymer into Layered Silicates in Real Time

KENNETH C. COLE*

Industrial Materials Institute, National Research Council Canada, Boucherville, Quebec, Canada J4B 6Y4

The intercalation of molten polymer into layered silicates (nanoclays) is a critical step in the fabrication of commercial polymer nanocomposite products, so it is therefore very important to understand the process of intercalation and exfoliation, as well as to properly characterize the final state achieved. Following on our recent work demonstrating the potential of transmission infrared spectroscopy for this purpose, we show in this work how the attenuated total reflection technique can be used to study the intercalation process in real time. Although various aspects of the Si-O stretching bands near 1150-950 cm^{-1} are sensitive to the intercalation, the most sensitive parameter is the relative intensity of the out-of-plane band near 1077 cm^{-1}. A method based on the second derivative of the spectrum has been developed to quantify this aspect. The application of this approach is described in detail and examples are given involving different polymers.

Index Headings: Nanocomposites; Nanoclay; Intercalation; Infrared Spectroscopy; Attenuated Total Reflection; Real Time; Layered Silicates; Polyethylene; Polystyrene; Polyamide-6.

* E-mail : kenneth.cole@imi.cnrc-nrc.gc.ca

INTRODUCTION

Polymer nanocomposites continue to attract a great deal of interest, because of the significant improvements in various properties that can be obtained when nanometric particles are well dispersed in a polymer matrix. The most common nanometric reinforcements are layered silicates or "nanoclays" like montmorillonite, which in their natural state consist of stacks of silicate layers about 1 nm thick. The achievement of good dispersion involves intercalation of the polymer into the space between the layers, ideally leading to complete separation of the layers, or exfoliation. It is therefore important to properly characterize the state of intercalation and exfoliation. Two techniques widely used for this purpose are X-ray diffraction and transmission electron microscopy, but even together they do not provide a complete picture. Recently, we showed that transmission infrared spectroscopy can provide very useful information on the state of intercalation and exfoliation, and it is therefore a valuable complement to these two techniques.[1] The key to its usefulness is the sensitivity of the Si-O stretching bands in the 1150-950 cm^{-1} region to the degree of intercalation. Although a detailed interpretation of this relationship is difficult to achieve, it is clear that a relationship exists and can be exploited. Further details on this relationship and the infrared spectra of layered silicates are given in Reference 1.

In this work we extend our earlier work to the attenuated total reflection technique, and show how it can be used to study clay intercalation by molten polymer in real time. We describe in detail the application of the technique and give examples involving different polymers. It should be noted that in these experiments the intercalation takes place under static conditions, not under shear as in the usual melt processing methods. However, it has been confirmed by means of X-

ray diffraction that, depending on the polymer and nanoclay, intercalation can readily occur under such static conditions.[2-5]

EXPERIMENTAL DETAILS

Spectrometer and ATR Accessory. The Fourier transform infrared spectrometer used was a Nicolet Magna 860 instrument from Thermo Scientific Canada (Mississauga ON), equipped with a DTGS detector. Spectra were recorded at a resolution of 4 cm^{-1} with an accumulation of 128 scans, requiring about 2.5 min. The ATR accessory used was a Golden Gate™ device from Specac Inc. (Cranston RI), equipped with zinc selenide lenses, a diamond reflection element, and a supercritical fluid top plate. This single-reflection accessory was chosen because it can be operated up to 300°C. The temperature was controlled by a 4000 Series™ controller, also from Specac. Because the high pressure used for supercritical fluid work was not required in this work, the standard pressure head was modified by Specac so that the inlet and outlet holes for high-pressure tubing were replaced by a single 5-mm hole in the center to expose the diamond element. The sample is placed in this hole and a 5-mm stepped plunger inserted to apply a small load. The modified top plate is illustrated in Fig. 1.

Materials. The following nanoclays were obtained from Southern Clay Products, Inc. (Gonzalez TX): Cloisite® Na^+ (sodium montmorillonite, without organic intercalant, d_{001} 1.17 nm), Cloisite® 15A (intercalated with 43 % by weight dimethyl di(hydrogenated tallow) quaternary ammonium, d_{001} 3.15 nm), and Cloisite® 20A (intercalated with 38% by weight of the same intercalant, d_{001} 2.42 nm).

The polymers used were: Polybond® 3009, a maleic-anhydride-grafted high-density polyethylene (HDPE) containing 1.0% maleic anhydride by weight, from Chemtura Corp.

(Middlebury CT); Polystyrene 1301, heat deflection temperature 93°C, from INEOS NOVA (Channahon IL); poly(styrene-*co*-maleic anhydride), $M_n \sim 1700$, styrene content 68 wt%, Cat. No. 442399, from Sigma-Aldrich Canada Ltd. (Oakville ON); and Ube 1015B2 polyamide-6, from Ube Industries Ltd. (Yamaguchi, Japan).

Procedure. The polymer to be used is first cryogenically ground, passed through a 180 μm sieve, and dried under appropriate conditions. It is then intimately mixed with the required amount of nanoclay with a mortar and pestle. A spectral background is recorded for the empty ATR accessory at ambient temperature. A small amount (about 20-30 mg) of the clay-polymer mixture is then deposited in the chamber of the ATR accessory, the plunger is inserted, and a small metal block is placed on top to add some extra pressure. A single-beam spectrum is then recorded at ambient temperature. Heating to a preset temperature is then commenced, and more single-beam spectra are recorded continuously while the temperature rises, then at suitable intervals once the preset temperature is reached. Spectra can also be recorded while the sample is cooling. At the end, the single-beam spectra are ratioed against the background recorded for the empty cell at ambient temperature. Because each spectrum requires about 2.5 min, the temperature can vary while it is being measured, and in such cases the range is noted.

Data Treatment. Basic spectral manipulation was performed with the OMNIC software provided with the Nicolet instrument. Peak fitting was performed with the use of GRAMS/AI software from Thermo Galactic Corp. Second derivatives were also calculated with this software, using the Savitsky-Golay algorithm with 13 data points and a polynomial of degree 2.

RESULTS AND DISCUSSION

Treatment of Spectra. Fig. 2 shows a typical spectrum, recorded at 190°C for Polybond 3009 containing 5 wt% Cloisite 20A. The reflectance spectrum has been converted into pseudoabsorbance units of $-\log_{10}R$, where R is the reflectance. The spectrum shows the usual polyethylene (PE) absorption bands around 3000-2800 cm^{-1}, 1500-1200 cm^{-1}, and 730 cm^{-1}, as well as the clay bands around 1200-800 cm^{-1}. However, there are other strong features in the 3800-3400 cm^{-1} and 2800-1600 cm^{-1} regions that arise from the diamond reflection element. These appear because the infrared transmission of the diamond varies with temperature, and the spectrum recorded at 190°C is ratioed against a background recorded for the empty cell at ambient temperature. Although these features do not interfere with the clay absorption bands, it is nevertheless desirable to eliminate them from the spectrum. To do this, a set of reference spectra were recorded for the empty cell at different temperatures and ratioed against the background recorded at ambient temperature, with the intention of subtracting these reference spectra from the sample spectra to eliminate the diamond features. The reference spectra are shown in Fig. 3a, where it is seen that the intensity of the cell signature increases monotonically with temperature. However, when the spectra are autoscaled, as shown in Fig. 3b, it is seen that the shape of the cell signature remains practically the same. This is important because it means that the temperature of the reference spectrum does not have to exactly match that of the sample spectrum. Instead, the closest reference spectrum can be chosen and the subtraction factor adjusted slightly to cancel out the diamond features. This is very useful when the sample temperature is not constant, for example in the case where the scans are accumulated while the temperature is increasing or decreasing.

Fig. 4 illustrates the overall spectral treatment procedure as applied to the spectrum of Fig. 2. Fig. 4a is the spectrum as recorded. Fig. 4b is the reference spectrum of the empty cell at 190°C. Fig. 4c shows the result obtained by subtracting the reference spectrum; the diamond features are completely eliminated. Fig. 4d is a similarly corrected spectrum of Polybond 3009 alone at 190°C. On subtracting this from the spectrum of the Polybond-clay mixture, the polymer peaks are eliminated and a clean spectrum of the clay is obtained for further analysis (Fig. 4e).

Polybond Experiment. Fig. 5 shows (from top to bottom) the "diamond-corrected" spectra obtained over the course of the complete Polybond experiment. The temperature was increased from ambient to 190°C over a period of about 20 min, maintained at 190°C for 30 min, allowed to decrease to ambient temperature over about 90 min, then increased again to 180°C. The initial spectrum, recorded at room temperature, is rather weak because at this point the mixture is in the form of discrete particles and makes good contact with the diamond surface only at specific points. Nevertheless, the clay peaks can be clearly seen at 1200-800 cm^{-1}, as well as weaker polyethylene peaks that show splitting because of the crystalline nature of the PE. The spectrum does not change until the temperature approaches the melting point of the Polybond (127°C), at which point the intensity begins to increase as the mixture softens and flows to make better contact with the diamond. Beyond the melting point the mixture wets the diamond surface completely and there is a significant increase in intensity. The crystalline splitting of the PE peaks disappears. As the temperature is maintained at 190°C for 30 min, the intensity of the PE peaks remains constant, but surprisingly, the intensity of the clay peak steadily diminishes. The reason for this is not clear, but it may be that preferential wetting of the diamond surface by the Polybond causes some migration of the clay particles away from the surface. As the sample is cooled, there is little change at first (170°C to 130°C), but below the melting point the crystalline

splitting starts to reappear. By the time the sample reaches room temperature, the spectrum is very weak, probably because shrinkage has caused the sample to pull away from the diamond surface and leave a gap. When the sample is remelted at 180°C, contact is re-established and the intensity of the PE peaks is the same as before cooling. The clay peak, however, is even weaker than before, possibly because transcrystallization at the interface upon cooling has forced the particles away from the diamond surface.

The main object of this experiment was to study the behavior of the clay peak. Clay spectra were generated by subtracting the spectrum of neat molten Polybond as described above. The evolution of the clay peaks during the experiment is shown in Fig. 6. Because of the overall intensity variation described above, to facilitate comparison of the spectra they have been normalized with respect to the peak maximum near 1040 cm^{-1}. As discussed in our earlier publication,[1] this peak is a composite peak involving four Si-O stretching vibrations, three of which (peaks I, III, and IV) have their transition moment in the plane of the clay platelets, and one of which (peak II) has its transition moment perpendicular to the plane. In a manner similar to that observed for the swelling of montmorillonites by water,[6] the shape of the band envelope changes as polymer intercalation occurs. In particular, peak II becomes much more prominent and the intensity ratio of peak III to peak IV increases somewhat. These trends are clearly evident in Fig. 6. They resemble those observed in our earlier work involving transmission measurements in the solid state on thin films of mixtures of pure PE with different amounts of Polybond 3009.[1] In that work, samples with different states of intercalation were obtained by processing of clay and polymer together in an extruder for different times.

Analysis of the Changes Observed. It is obviously of interest to correlate the changes observed with the state of intercalation in some quantitative manner. In our earlier work, we

adapted the peak-fitting approach used by Yan et al. for water swelling.[6] Unfortunately, a detailed analysis of the band envelope and rigorous peak fitting are difficult to achieve, owing to the complexity of the situation. Even in their pristine state, montmorillonites are natural materials and do not possess a perfect crystalline structure but rather a distribution of somewhat imperfect structures. Intercalation further broadens this distribution, as different clay stacks may be intercalated to different extents. As a result, the IR absorption bands do not show a perfectly Lorentzian shape but include some Gaussian character, the degree of which may vary, and they may even be asymmetric. This makes rigorous peak fitting very difficult. Despite this, we were able to develop an approach that worked reasonably well,[1] and works equally well in the case of the ATR spectra obtained here, as illustrated in Fig. 7. In this approach, the main clay peak is resolved into six peaks with a Pearson VII line shape. To obtain an acceptable fit, it was necessary to use two components (IIIa and IIIb) for peak III and to introduce a broad underlying peak ("peak V") whose significance is not fully understood. As was the case for the study of water swelling by Yan et al.,[6] the parameter most sensitive to the degree of intercalation was found to be the position of peak II. The variation of this parameter with time is shown in Fig. 8, with time zero defined as the point at which the temperature exceeds the polymer melting point. The position of peak II increases smoothly with time over a significant range of about 15 cm^{-1}. This behavior is similar to that observed in our previous work in transmission, except that the variation is smoother because all the spectra were measured *in situ* on the same sample, rather than on a series of separate samples prepared with different processing times. Over the period in which the polymer is in the molten state, the variation of peak II can be well fitted by an exponential rise, as shown in Fig. 8.

Although the peak fitting approach is acceptable, we also explored an alternative approach that is often used to resolve the details of infrared spectra, namely the use of the second derivative. Taking the negative second derivative results in narrowing of a Lorentzian or Gaussian peak, but introduces negative wings on either side. Fig. 9 shows the negative second derivatives of the spectra shown in Fig. 6. The first observation is that the four Si-O stretching vibrations between 1140 and 980 cm^{-1} are now fairly clearly resolved, and there is no indication of other distinct peaks in this region. The second, rather important, observation is the pronounced growth of the out-of-plane peak II with time. Initially it is barely present, and it changes little until the polymer melts, at which point it grows significantly with respect to the other peaks. The ratio of peak III to peak IV also increases somewhat with time. In addition, shifts in peak positions are evident, particularly for peaks I and III, whose variation seems to follow the variation in temperature. Peak I moves from 1116 cm^{-1} at room temperature to 1111 cm^{-1} at 190°C, peak III from 1050 cm^{-1} to 1043 cm^{-1}, and peak IV from 1012 cm^{-1} to 1016 cm^{-1}. For peak II, it is difficult to determine an accurate position in the early stages, where it is weak; when it is strong, it occurs at 1077 cm^{-1}.

The question arises as to what extent these changes are due simply to the change in temperature rather than intercalation of the polymer. To explore this aspect, a sample of neat Cloisite 20A clay in powder form was placed in the cell and the spectrum measured as the temperature was increased step-wise from ambient to 200°C, with each temperature being maintained for about 10 min, long enough to acquire 128 scans at constant temperature. The resulting normalized absorbance spectra are shown in Fig. 10a and their second derivatives are shown in Fig. 10b. The most striking observation is that, in contrast with Figs. 6 and 9, no growth whatsoever is observed for peak II. It cannot be detected in the absorbance spectra but is

seen as a weak and stable feature in the second derivative spectra. A second observation is that the other peaks change position linearly with temperature on heating from ambient temperature to 200°C, from 1117 cm^{-1} to 1111 cm^{-1} for peak I, 1053 cm^{-1} to 1045 cm^{-1} for peak III, and 1013 cm^{-1} to 1007 cm^{-1} for peak IV. For peaks I and III, these shifts are similar to those seen in Fig. 9, but for peak IV the shift is in the opposite direction. Furthermore, the intensity ratio of peak III to peak IV decreases with temperature, whereas in Fig. 9 it increases. It is clear that the behavior of the Si-O stretching peaks is very complex and that both temperature and intercalation affect them. Further work is required to interpret the behavior fully. However, it is also clear that the growth of peak II is related to the state of intercalation and not to temperature effects. The temperature effects are no doubt due to the expansion of the silicate network on heating. Loo and Gleason have shown by means of peak fitting that the Si-O bands at 1046 cm^{-1} and 1018 cm^{-1} in polyamide-6/montmorillonite nanocomposites also shift to lower frequency when the nanocomposites are subjected to mechanical strain.[7]

Further insight into the behavior was gained by performing a similar experiment with Cloisite Na^+. In this clay, which more closely resembles natural montmorillonite, the interlayer galleries are occupied by Na^+ ions surrounded by hydrating water molecules, rather than by the long-chain-hydrocarbon quaternary ammonium ion intercalant found in Cloisite 20A. The spectra obtained are shown in Fig. 11. The absorbance spectra (Fig. 11a) appear rather similar to those of Cloisite 20A, although the overall band envelope is significantly broader. However, the second derivative spectra (Fig. 11b) show that these spectra are deceptively simple and that the situation is more complex. The room temperature spectrum shows peak I at 1119 cm^{-1}, possibly a very weak peak II around 1090 cm^{-1}, peak III at 1045 cm^{-1}, and peak IV at 1001 cm^{-1}. As in the case of Cloisite 20A, peaks I, III, and IV all move to lower frequency on heating. The most

striking change, however, is the growth of two peaks near 1056 cm^{-1} and 1015 cm^{-1}, which grow mainly over the range of 70°C to 120°C. The reason for this is a sort of "reverse intercalation" corresponding to the loss of water from the interlayer galleries. Confirmation of this is provided by Fig. 12, which shows the 1800-1300 cm^{-1} region of the spectra shown in Fig. 11a. The water bending mode peak at 1637 cm^{-1} decreases upon heating, with the decrease especially apparent over the range 70°C to 120°C. (The invariant peak at 1500-1400 cm^{-1} is probably due to carbonate ion present as an impurity in the montmorillonite.) Thus, the sodium montmorillonite spectra can be considered to correspond to a superposition of two intercalation states – one with water (peaks III and IV near 1045 and 1001 cm^{-1} respectively) and one without (peaks III and IV near 1056 and 1015 cm^{-1}). It should be noted that the exact positions of these peaks are subject to some imprecision because of their overlap as well as the effect of temperature.

A further point of discussion is the fact that, according to the second derivative spectra of Fig. 9, the position of peak II does not change much as a function of intercalation. This is contrary to our earlier conclusion,[1] as well as that of Yan et al.,[6] which indicated, based on peak fitting, that peak II shifts to significantly higher wavenumber upon intercalation. There is, however, a possible explanation of this discrepancy. It may be that in the initial less intercalated state, peak II occurs at sufficiently low wavenumber that it overlaps closely with peak III and is not clearly resolved in the peak fitting procedure. The second derivative, on the other hand, can resolve the two components of peak II, namely the higher-wavenumber component corresponding to the more highly intercalated state and the lower-wavenumber component corresponding to the less intercalated state, although the latter cannot be detected in the second derivative spectra because it is too close to peak III to be resolved. In the peak fitting procedure, the two components are merged into a single peak. As the lower-wavenumber component

decreases and the higher-wavenumber component increases, the merged peak will show an apparent shift to higher wavenumber. This explanation has been proposed by Tzavalas and Gregoriou, who measured the transmission spectra of thin films of a nanocomposite based on melt-mixed high-density polyethylene (without anhydride modification) and Cloisite 20A.[8] Based on peak fitting, they concluded that the clay spectrum can be regarded as a superposition of two intercalation states, one of which corresponds to the starting Cloisite 20A, with peaks at 1070 and 1050 cm^{-1}, and the other to HDPE-intercalated clay, with the same peaks shifted to 1085 and 1040 cm^{-1}. As intercalation proceeds, the latter two peaks grow at the expense of the former two. Like the peak fitting procedure developed in our previous work,[1] the one used by Tzavalas and Gregoriou is imperfect, because of the complexity of the Si-O stretching bands. However, the present results provide support for their conclusions and their concept of two distinct intercalation states.

For the second-derivative spectra of Fig. 9, quantification of the growth of peak II was done as shown in Fig. 13. Peak heights were calculated with respect to the minimum value of the curve near 1060 cm^{-1}. The ratios of the height of peak II with respect to peaks III and IV are plotted in Fig. 14. Both the II/III and II/IV ratios show a smooth evolution similar to that observed for the position of peak II from the peak fitting (Fig. 8), and both can be fitted well by an exponential rise. Either one could be used to quantify the changes. The use of a second-derivative ratio has definite advantages over the peak fitting procedure. Firstly, it is much simpler to calculate. Secondly, a value can be determined even in the early stages of intercalation, where it is difficult to resolve peak II by the peak fitting procedure. The peak heights can also be calculated with respect to zero rather than the minimum value. The peak height ratios calculated in this way show the same pattern of variation with intercalation as in

Fig. 14, but this method has the disadvantage of giving negative values of the height of peak II in the early stages.

Examples Involving Other Polymers. Figures 15 to 17 show that the ATR method can be applied equally well to a variety of polymers. When the polymer possesses strong absorption peaks, they do not always cancel out completely upon subtraction of the neat polymer spectrum, because interaction with the clay can lead to slight changes in the peak positions and/or shapes. This occurs at 1500-1400 and 800-650 cm^{-1} in polystyrene (Fig. 15) and at 1700-1400 cm^{-1} in polyamide-6 (Fig. 16). As long as there are no strong peaks in the clay absorption region of 1200-800 cm^{-1}, this does not present problems. However, a polymer with a high maleic anhydride content like the poly(styrene-*co*-maleic anhydride) of Fig. 17 possesses strong peaks in the clay region and care must be exercised in interpreting the resulting clay spectra. It is interesting to note the variation in the shape of the clay peak envelope with the polymer matrix in the examples of Figs. 15-17. More detailed studies involving different polymers and nanoclays will be reported in future publications.

CONCLUSIONS

Infrared spectroscopy in the attenuated total reflection mode is a very useful technique for monitoring *in situ* the intercalation of different molten polymers into montmorillonite-based nanoclays. The key parameter is the significant growth of the out-of-plane Si-O stretching vibration (peak II) with respect to the in-plane vibrations (peaks I, III, and IV). This growth can be easily quantified by taking the negative second derivative of the clay spectra and calculating the ratio of the height of peak II with respect to peak III or peak IV.

ACKNOWLEDGEMENT

The careful work of Dominique Desgagnés in recording the infrared spectra is gratefully acknowledged. Thanks are also due to Dr. Spiros Tzavalas for providing helpful discussion and information.

REFERENCES

1. K. C. Cole, Macromolecules **41**, 834 (2008).
2. R. A. Vaia, K. D. Jandt, E. J. Kramer, and E. Giannelis, Macromolecules **28**, 8080 (1995).
3. N. Hasegawa and A. Usuki, J. Appl. Polym. Sci. **93**, 464 (2004).
4. Y. Li and H. Ishida, Macromolecules **38**, 6513 (2005).
5. S. Filippi, C. Marazzato, P. Magagnini, A. Famulari, P. Arosio, and S. V. Meille, Eur. Polym. J. **44**, 987 (2008).
6. L. Yan, C. B. Roth, and P. F. Low, Langmuir **12**, 4421 (1996).
7. L. S. Loo and K. K. Gleason, Macromolecules **36**, 2587 (2003).
8. S. Tzavalas and V. G. Gregoriou, "Infrared Spectroscopy as a Tool to Monitor the Extent of Intercalation and Exfoliation in Polymer Clay Nanocomposites", Vib. Spectrosc., in press.

LIST OF FIGURES

Fig. 10. Evolution with temperature of (a) the normalized absorbance spectra of neat Cloisite 20A and (b) the negative second derivative curves of the same spectra.

Fig. 11. Evolution with temperature of (a) the normalized absorbance spectra of neat Cloisite Na^+ and (b) the negative second derivative curves of the same spectra.

Fig. 12. Evolution with temperature of the water bending mode peak in the normalized absorbance spectra of neat Cloisite Na^+.

Fig. 13. Illustration of the method for calculating peak height ratios in the second derivative spectra of Figure 9.

Fig. 14. Evolution of the peak height ratios as a function of time in the molten state for the spectra of Fig. 9. The dashed and dotted lines correspond to an exponential rise fit.

Fig. 15. (a) Spectrum of Polystyrene 1301 + 5% Cloisite 20A at 160°C, corrected for the effect of temperature on the empty cell; (b) Similarly corrected spectrum of Polystyrene 1301 alone; (c) Clay spectrum obtained by subtracting b from a. Spectra are offset along the y-axis for clarity.

Fig. 16. (a) Spectrum of Ube 1015B2 polyamide-6 + 2% Cloisite 15A at 240°C, corrected for the effect of temperature on the empty cell; (b) Similarly corrected spectrum of Ube 1015B2 polyamide-6 alone; (c) Clay spectrum obtained by subtracting b from a. Spectra are offset along the y-axis for clarity.

Fig. 17. (a) Spectrum of PS-*co*-MA + 5% Cloisite 20A at 190°C, corrected for the effect of temperature on the empty cell; (b) Similarly corrected spectrum of PS-*co*-MA alone; (c) Clay spectrum obtained by subtracting b from a. Spectra are offset along the y-axis for clarity.

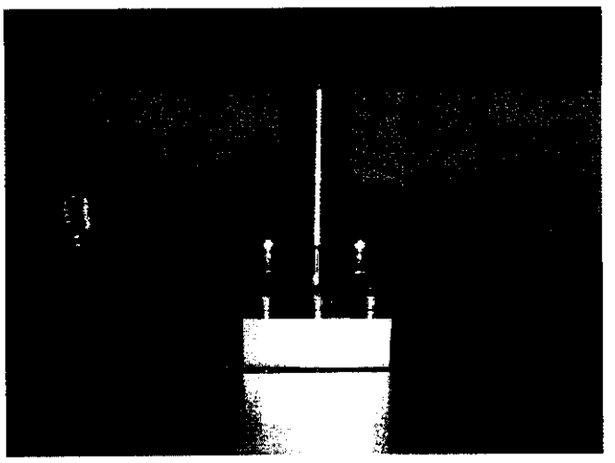

Fig. 1. Photograph of modified top plate of Golden Gate accessory.

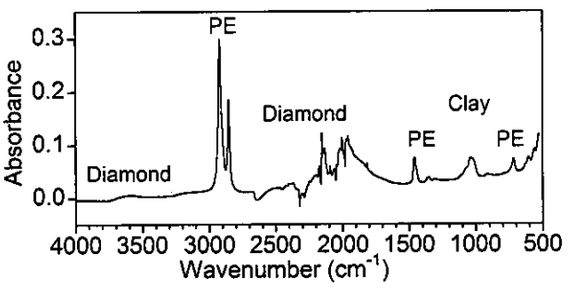

Fig. 2. Typical spectrum of Polybond 3009 containing 5% Cloisite 20A, recorded at 190°C.

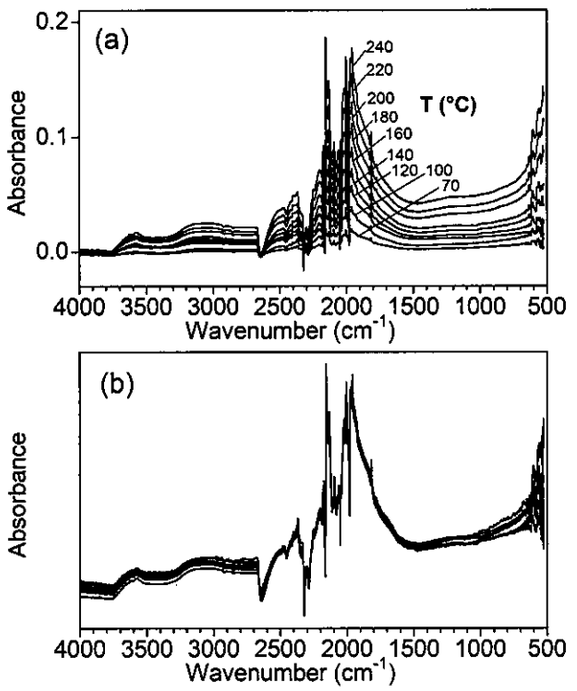

Fig. 3. (a) Reference spectra of empty Golden Gate accessory recorded at different temperatures, ratioed against ambient temperature; (b) The same spectra after autoscaling.

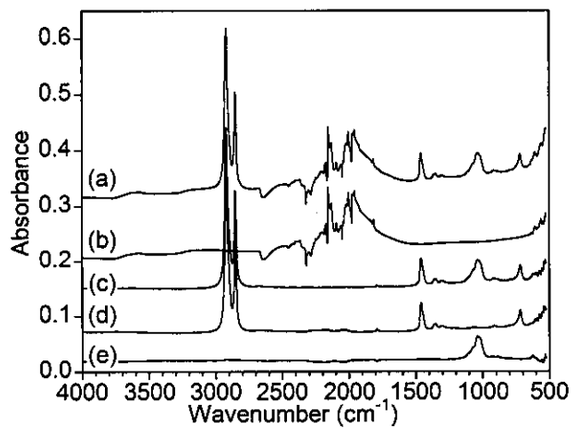

Fig. 4. (a) Spectrum of Polybond 3009 + 5% Cloisite 20A at 190°C, recorded with ambient-temperature empty cell as background; (b) Reference spectrum of empty cell at 190°C; (c) Corrected spectrum obtained by subtracting b from c; (d) Similarly corrected spectrum of Polybond 3009 alone; (e) Clay spectrum obtained by subtracting d from c. Spectra are offset along the y-axis for clarity.

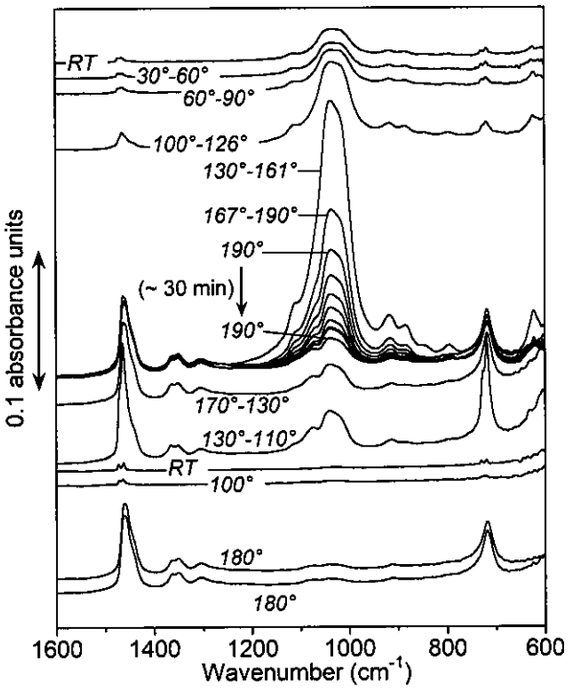

Fig. 5. From top to bottom: spectra recorded during experiment involving Polybond 3009 + 5% Cloisite 20A, heated from ambient temperature to 190°C, maintained at 190°C for 30 min, then cooled to ambient temperature and reheated to 180°C. Spectra are offset along the y-axis for clarity.

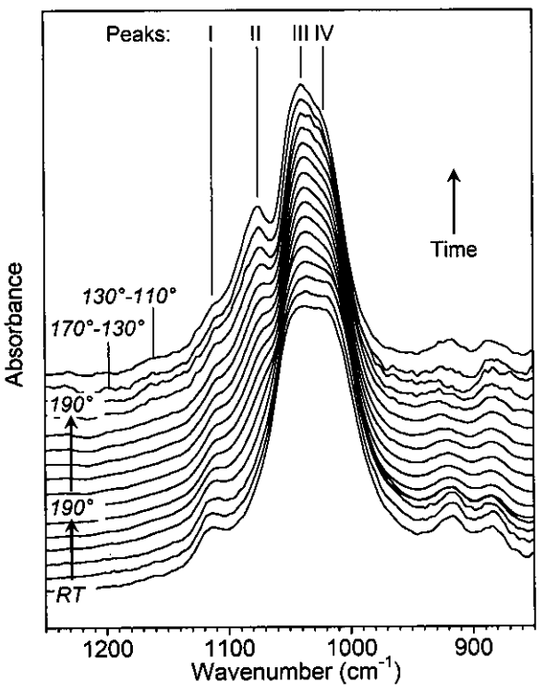

Fig. 6. Evolution of the clay peaks during the experiment of Fig. 5.

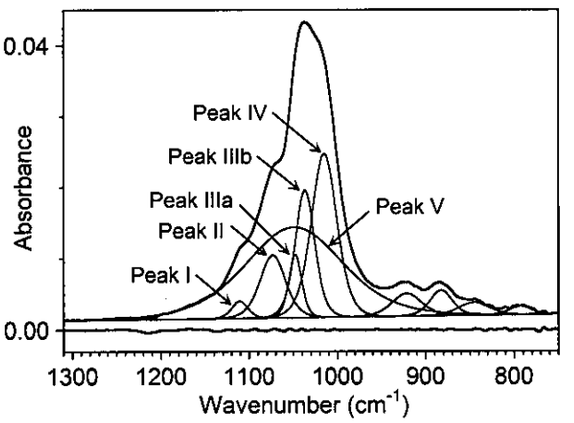

Fig. 7. Peak fitting of the clay peaks from a spectrum recorded at 190°C. The wavy line at the bottom corresponds to the residual difference between the experimental curve and the fit envelope.

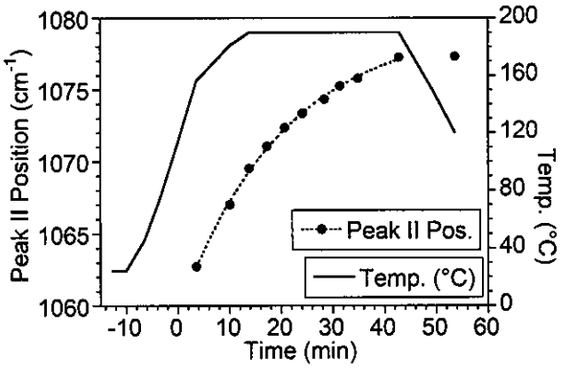

Fig. 8. Evolution of the position of Peak II (solid circles) as a function of time in the molten state. The dotted line corresponds to an exponential rise fit. The solid line shows the variation of temperature.

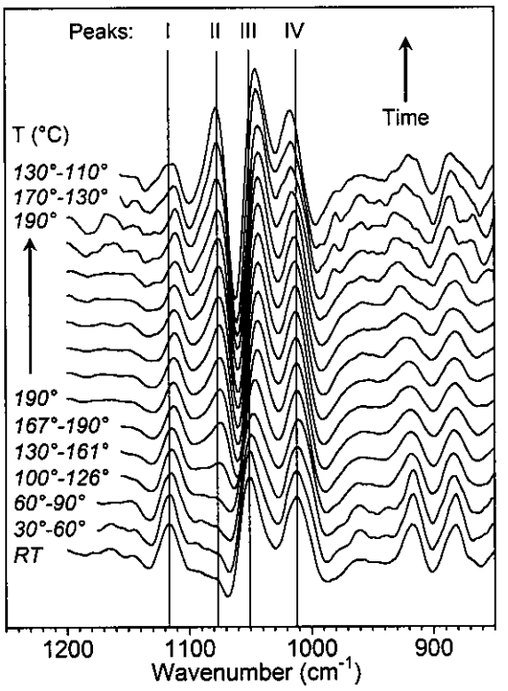

Fig. 9. Evolution with time and temperature of the negative second derivative curves of the clay spectra shown in Fig. 6.

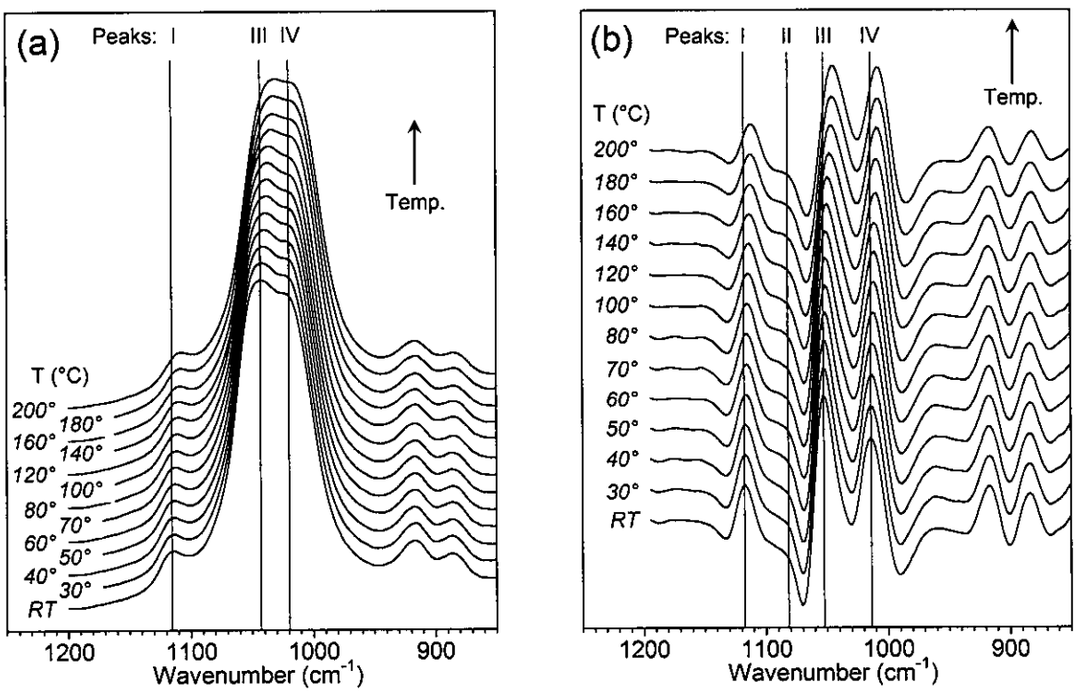

Fig. 10. Evolution with temperature of (a) the normalized absorbance spectra of neat Cloisite 20A and (b) the negative second derivative curves of the same spectra.

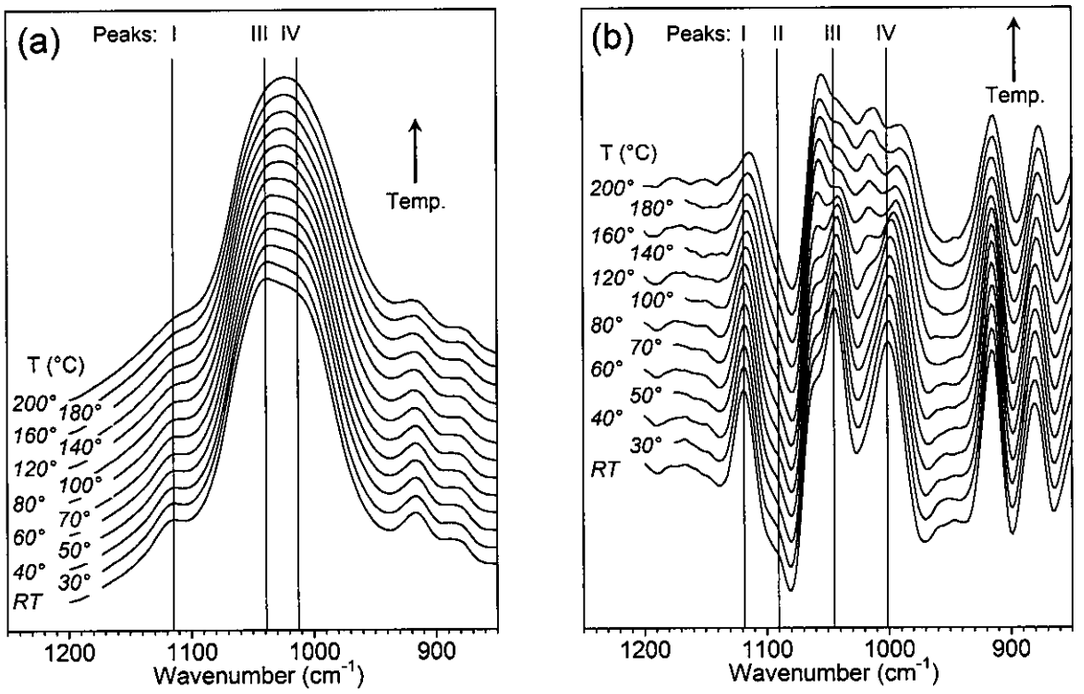

Fig. 11. Evolution with temperature of (a) the normalized absorbance spectra of neat Cloisite Na^+ and (b) the negative second derivative curves of the same spectra.

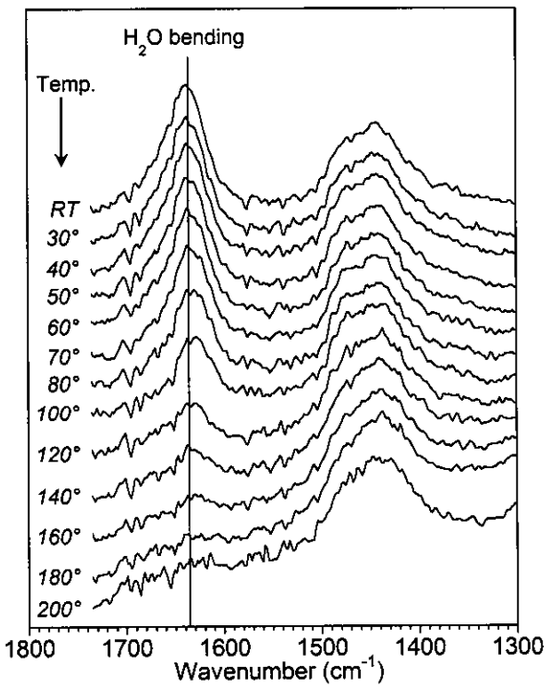

Fig. 12. Evolution with temperature of the water bending mode peak in the normalized absorbance spectra of neat Cloisite Na^+.

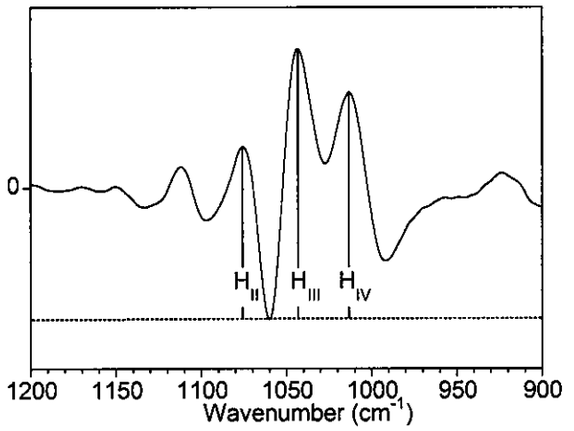

Fig. 13. Illustration of the method for calculating peak height ratios in the second derivative spectra of Figure 9.

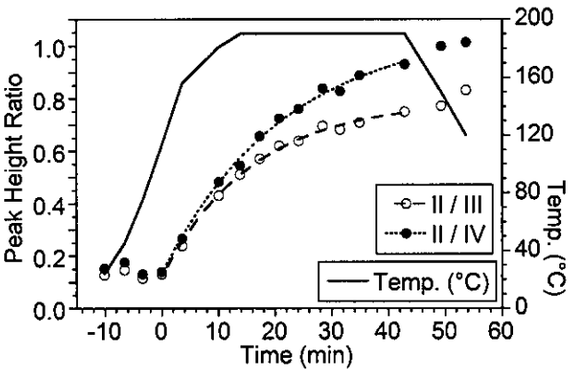

Fig. 14. Evolution of the peak height ratios as a function of time in the molten state for the spectra of Fig. 9. The dashed and dotted lines correspond to an exponential rise fit.

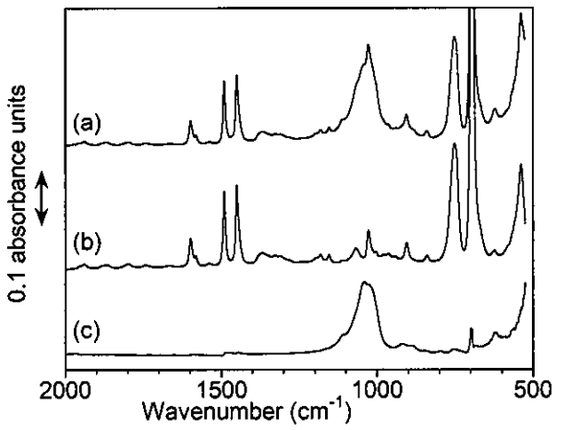

Fig. 15. (a) Spectrum of Polystyrene 1301 + 5% Cloisite 20A at 160°C, corrected for the effect of temperature on the empty cell; (b) Similarly corrected spectrum of Polystyrene 1301 alone; (c) Clay spectrum obtained by subtracting b from a. Spectra are offset along the y-axis for clarity.

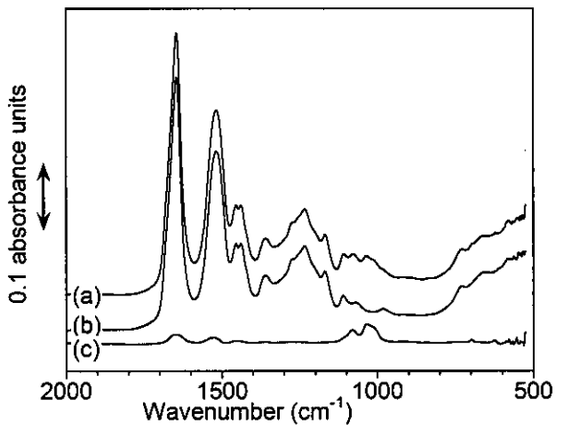

Fig. 16. (a) Spectrum of Ube 1015B2 polyamide-6 + 2% Cloisite 15A at 240°C, corrected for the effect of temperature on the empty cell; (b) Similarly corrected spectrum of Ube 1015B2 polyamide-6 alone; (c) Clay spectrum obtained by subtracting b from a. Spectra are offset along the y-axis for clarity.

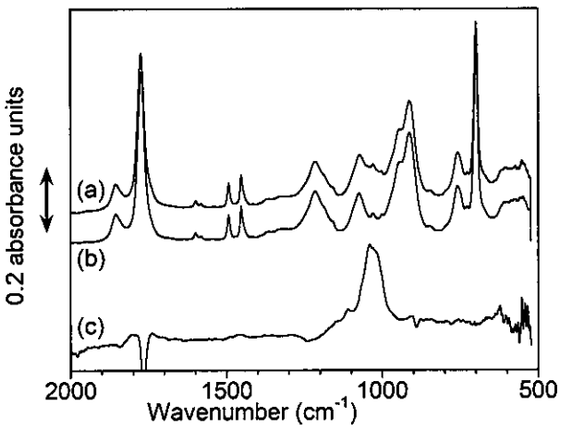

Fig. 17. (a) Spectrum of PS-*co*-MA + 5% Cloisite 20A at 190°C, corrected for the effect of temperature on the empty cell; (b) Similarly corrected spectrum of PS-*co*-MA alone; (c) Clay spectrum obtained by subtracting b from a. Spectra are offset along the y-axis for clarity.